## Book Chapter

# Effect of Angle between Pier and Center of River Flow on Local Scouring around the Bridge Pier

Takuma Kadono[1], Shinichiro Okazaki[2]*, Yoshihiro Kabeyama[1] and Toshinori Matsui[2]

[1]Graduate School of Engineering, Kagawa University, Japan
[2]Faculty of Engineering and Design, Kagawa University, Japan

***Corresponding Author:** Shinichiro Okazaki, Faculty of Engineering and Design, Kagawa University, Takamatsu, Kagawa 761-0396, Japan

Published **February 18, 2021**

This Book Chapter is a republication of an article published by Shinichiro Okazaki, et al. at Water in November 2020. (Kadono, T.; Okazaki, S.; Kabeyama, Y.; Matsui, T. Effect of Angle between Pier and Center of River Flow on Local Scouring around the Bridge Pier. Water 2020, 12, 3192. https://doi.org/10.3390/w12113192)

**How to cite this book chapter:** Takuma Kadono, Shinichiro Okazaki, Yoshihiro Kabeyama, Toshinori Matsui. Effect of Angle between Pier and Center of River Flow on Local Scouring around the Bridge Pier. In: Tewodros Tena, editor. Water: Ecology and Management. Hyderabad, India: Vide Leaf. 2021.



**Author Contributions:** Conceptualization, T.K. and S.O.; methodology, T.K. and T.M.; validation, T.K. and S.O.; formal

analysis, T.K. and S.O.; investigation, T.K. and Y.K.; resources, S.O. and T.M.; data curation, T.K. and Y.K.; writing—original draft preparation, T.K.; writing—review and editing, Y.K. and T.M.; visualization, Y.K.; supervision, S.O.; project administration, T.K.; funding acquisition, S.O. All authors have read and agreed to the published version of the manuscript.

**Funding:** This research was supported by the Ministry of Land, Infrastructure, Transport and Tourism, Construction Technology Research and Development Grant Program (CRD).

**Acknowledgments:** We received kind cooperation from the Railway Technical Research Institute in Japan in order to access the details of the case of the disaster that this study is focused on. This research was supported by the Ministry of Land, Transport and Tourism, Construction Technology Research and Development Grant Program (CRD). We also would like to thank the MDPI author service for English language editing. We would like to express our gratitude to them.

**Conflicts of Interest:** The authors declare no conflict of interest.

## Abstract

In recent years, heavy rainfall disasters have caused frequent damage to bridge piers due to scouring and have resulted in the fall of bridges in many areas in Japan. The objective of this study was to investigate the effect of local scouring around the downstream of the piers on the local scouring around the center of the river flowing at an angle to the piers. It was found that when the center of the river flows at an angle to the piers, the scouring area becomes wider from the upstream to the downstream of the piers because of the longer inhibition width of the piers positioned perpendicular to the water flow. The downstream scouring depth tends to be smaller than the upstream scouring depth. In addition, the time to the onset of tilting deformation of the piers increases with the inhibition width of the piers positioned perpendicular to the flowing water.

## Keywords

Pier; Local Scouring; Tilting Deformation Of Bridge Pier; Central River Flow; Inhibition Width

## Introduction

In recent years, heavy rainfall disasters have caused frequent damage to bridge piers due to scouring and have resulted in the fall of bridges in many areas of Japan, e.g., in July 2017, when the collapse of piers and outflow of girders of a railway bridge occurred due to heavy rainfall in the northern part of the Kyushu area. In July 2018, the inclination of a pier and outflow of girders of a railway bridge were caused by heavy rainfall in western Japan. In addition, in July 2020, the collapse of piers and outflow of girders of a railway bridge were caused by heavy rainfall in the southern part of the Kyushu area. When this type of disaster occurs, it has a significant impact on the transportation network and on the daily lives of people. In particular, old-fashioned piers with a shallow embedded depth and direct foundation often undergo damage due to local scouring around the piers. Therefore, it is necessary to clarify the safety and soundness of the foundations regularly. In Japan, the Ministry of Land, Infrastructure, Transport and Tourism requires regular inspection of once every two years for railways and once every five years for roads. However, it is difficult for an engineer engaged in the maintenance practice of bridges to actually perform a detailed investigation for the purpose of clarifying the safety and soundness on a daily basis because there are many aspects that require maintenance. Therefore, it is common to conduct a simple investigation based on visual methods and by using a tape measure.

Samizo [1] proposed a method to evaluate the risk of local scouring around piers based on the data of existing disasters by using a multivariate model with several parameters that can be obtained in maintenance practice. This method allows easy and efficient bridge maintenance. Keyaki [2] proposed a method to evaluate the natural frequency of piers by the measurement of fine movement using sensors installed on both edges at the top of the pier against its axis direction. Furthermore, in recent years, a

research study has been conducted on a method for evaluating possibility of bridge pier scouring based on evaluating river hydrological events, modeling river behavior and estimating the scour depth [3]. This can enable constant monitoring of the soundness of the pier.

Several researchers [4–13] have proposed formulae for evaluating the scour depth, which is important for evaluating the safety of piers. Engineers engaged in maintenance practice use these formulae to evaluate the risk of local scouring around piers. Although there is previous study on the conditions that occur when a pier is scoured in the downstream direction [4], in most studies, the shape of the scour hole is assumed to be inverted conical with upstream water flow direction.

In this study, we focused on the July 2018 disaster in Japan. Heavy rainfall occurred, and a pier was damaged after being tilted towards the downstream and right bank side directions. The cause of the tilting of the pier was assumed to be scouring of the area of the downstream and right bank side around the pier based on its tilting direction. In this study, we provide an overview of the case focused on the disaster. We conducted experiments using a scale model to clarify the condition of occurrence of local scouring in the downstream direction around the pier and the effect on the progressof local scouring.

## Overview of the Disaster

The case is focused on a railway bridge, specifically an inclined fourth pier (4P) due to river flooding from the heavy rainfall of the July 2018 disaster in Japan. In this case, train operations were obstructed for approximately a month because of horizontal displacements at the tracks affected by the 4P inclination. The extent of the damage is shown in Figures 1 and 2, and an overall view of the damaged bridge is shown in Figure 3. The damaged bridge was a railway bridge with a total length of 137.19 m, composed of seven steel deck plate girders with a span of 19.2 m and six piers and two abuts of direct foundation type that were constructed by stonemasonry. The superstructure weight per pier was approximately 300 kN, considering the sidewalk of the bridge, which had an incidental structure and an approximate track weight similar to that of the rails. The basin area of the

river in which the bridge was damaged was 155.5 $km^2$. The damaged bridge was constructed in 1913 and was previously repaired at the third (3P) and fifth (5P) piers by the manager of the structure. Concrete lining was installed at 3P and foot protection works were performed at 5P. In addition, the embedded depth of 4P was measured as 0.9 m during June 2017, before the disaster. The embedded ratio, which is the ratio of the embedded depth and the pier width in the transverse direction against the pier axis, was calculated to be 0.46.

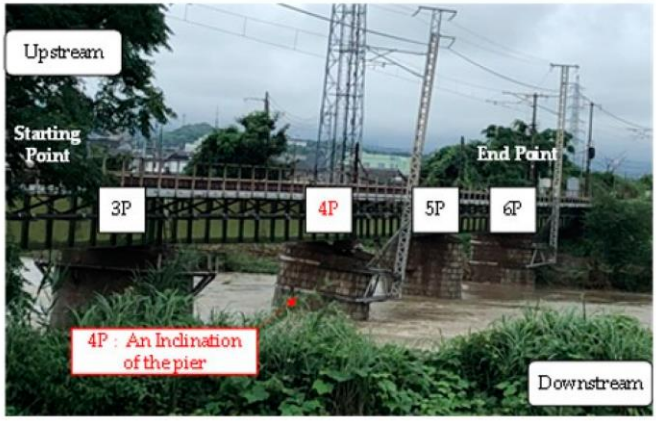


**Figure 1:** Overall damage.

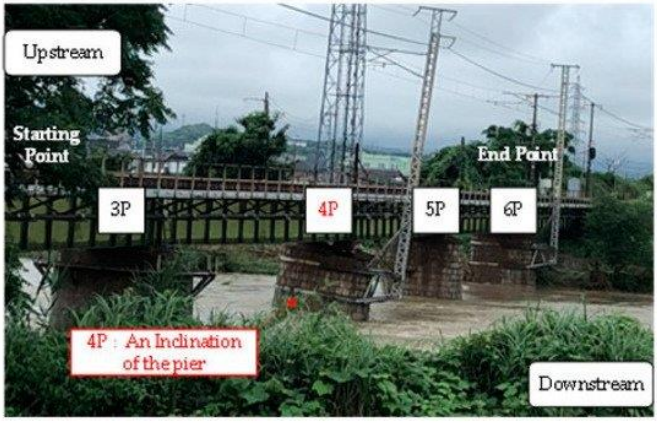


**Figure 2:** Damage to the tracks.

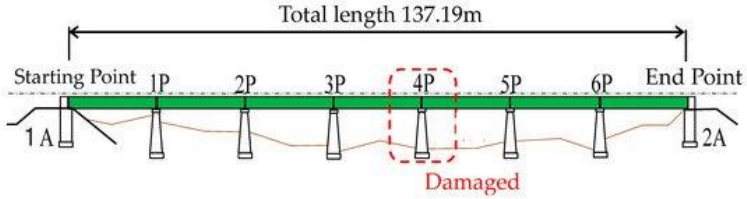


**Figure 3:** Overall view of the damaged bridge.

On 7 July 2018, 4P was inclined towards the downstream and the right bank side direction due to local scouring around it due to river flooding. As a result, the tracks were horizontally displaced 752 mm towards the downstream direction, and train operations were performed with restrictions.

According to a rain gauge located near the damaged bridge, 378 mm of continuous rainfall occurred, and the maximum rainfall per hour was 28 mm. The inclination angle of 4P was estimated to be approximately 50/1000 rad based on the horizontal displacement that occurred at the tracks. Although 4P was inclined, cracks did not develop in the joints of the stone foundations. However, the downstream bearings slipped out from the pier, and the upstream bearings were damaged so that the soleplates were deformed, and some rivets were loosened.

According to the results of the impact vibration examination performed by the manager of the structure, the natural frequency of 4P at the time of the damage was 4.9 Hz. We confirmed that the natural frequency at the time of the damage was lower than 9.3 Hz, similar to the natural frequency during June 2017, before the disaster. In addition, we confirmed that the natural frequency at the time of the disaster was lower than 9.2 Hz, similar to the standard value of the natural frequency, which can be calculated by the formula provided in the maintenance standard (railway structure edition, foundation structure and retaining structure) [14].

A topographical map of the damaged bridge is shown in Figure 4. This topographical map was generated using Blender, which is a general-purpose physics simulator, by using Standard Triangle Language data, obtained from the Geospatial Information

Authority of Japan. We can confirm that the bridge had an angle against the center of the river flow because the river flow was curved from upstream. Therefore, the center of the river flow at the time of river flooding was flowing at an angle of approximately 45° against the damaged bridge. We considered this as the cause of damage to 4P, which was inclined in the downstream and right bank side directions by the angle.

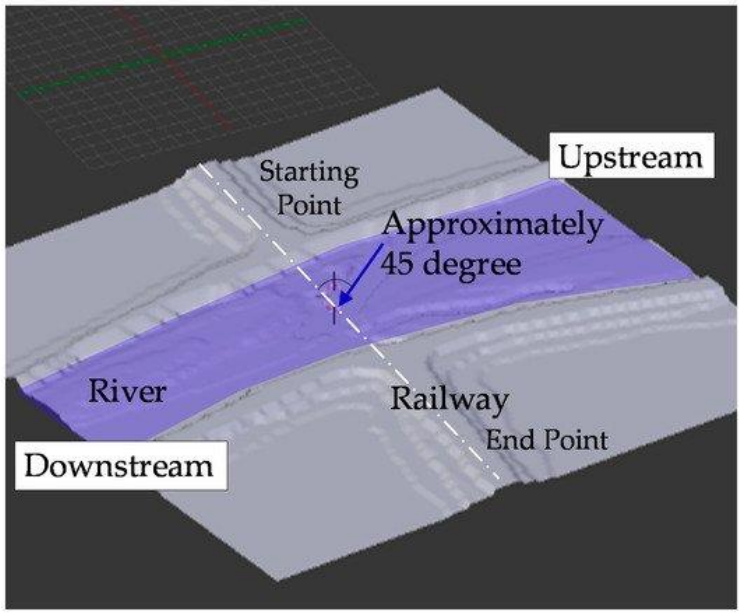


**Figure 4:** Topographical map of the damaged bridge.

## Outline of Experiments

### Experimental Conditions

We performed water flow experiments using a scale model of the pier. The aim of this experiment was to clarify the condition of local scouring of the pier in the downstream direction. The scale model, which was rotated at an angle $\theta$ against the center of the water flow (C.L.), was installed at the center of a soil layer, as shown in Figure 5a. This was because the center of the river flow was required to flow at a particular angle against the pier.

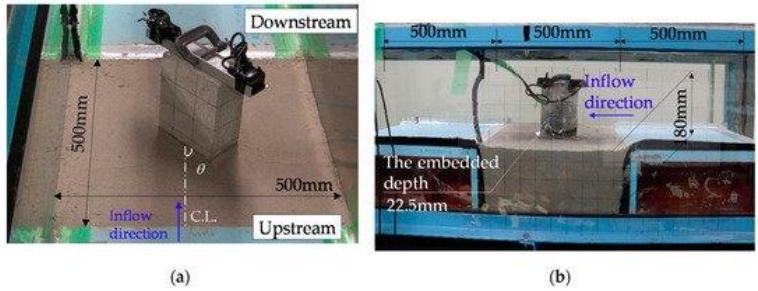


**Figure 5:** Outline of the experiment using a scale model: (**a**) front view; (**b**) side view.

The scale model was constructed using mortar and was rectangular with a short side of 76.3 mm, long side of 136.3 mm and height of 198.8 mm (weight 4.48 kg). The scale of the model was 1/40 to the actual scale of the damaged bridge. A 1500 mm long and 500 mm wide flume was used in the experiments with open channel equipment. A soil layer with a width of 500 mm, length of 500 mm and depth of 180 mm was constructed at the center of the flume by raising a waterbed around the soil layer at 180 mm using H-section steel (height 150 mm) and polystyrene foam (thickness 30 mm). The embedded depth was 22.5 mm, and silica sand no. 7 was spread evenly in the soil layer. The embedded depth of the scale model was defined based on that of 4P before the disaster. In addition, a weight of 0.5 kg, which simulated the superstructure, was installed on top of the scale model. The weight was roughly similar to that of the actual superstructure because it could be converted to 313.7 kN based on the assumption that it was equal to the Froude number of the actual structure and the scale model.

## Experimental Cases

Here, we present the experiments performed using the scale model shown in Table 1. The experiments were performed as follows. First, the water was flowed in slowly towards the surface of the soil layer. Afterwards, it was flowed in at a fixed flow rate. In addition, the height of the water flow and its velocity was converted to 1.156 from 0.724 m and to 2.403 from 1.581 m/s, respectively, at the actual scale.

**Table 1:** Cases of experiments using the scale model.

| Case | $\theta$ (degree) | Water Height (m) | Velocity (m/s) | $F_r$ |
|---|---|---|---|---|
| Case 1 | 0 | 0.0181 | 0.38 | 0.90 |
| Case 2 | 45 | 0.0248 | 0.30 | 0.61 |
| Case 3 | 0 | 0.0238 | 0.30 | 0.62 |
| Case 4 | 30 | 0.0230 | 0.31 | 0.65 |
| Case 5 | 45 | 0.0289 | 0.25 | 0.47 |

$F_r$ is the Froude number.

The angles in cases 1 and 2 were $0^o$ and $45^o$, respectively. We measured the shape of the scour before the inclination of the scale model 60 and 360 s after reaching the surface of the soil layer in cases 1 and 2, respectively. We compared cases 1 and 2 in terms of the fluctuation of the scouring region due to the angle between the pier and the center of the water flow and the effect of the angle on scouring. The angles in cases 3, 4 and 5 were $0^o$, $30^o$ and $45^o$, respectively. In cases 3–5, the inflow was continued until the scale model inclined and was unable to stand on its own due to local scouring as shown in Figure 6. We clarified the effect on the initiation tendency for the inclination of the pier due to local scouring affected by the angle based on the results of these experiments.

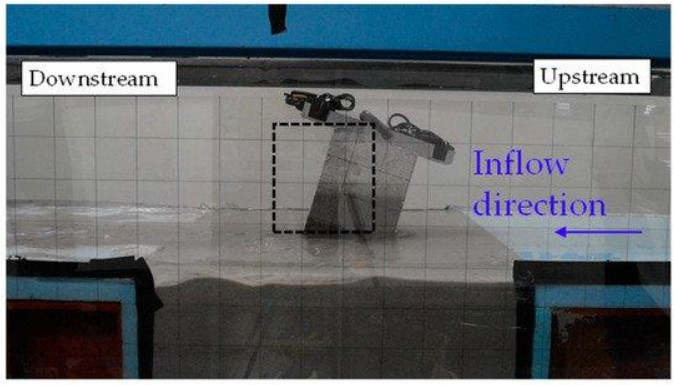


**Figure 6:** An example of the scale model that was unable to stand on its own (case 3).

To conduct measurements at the time of the experiment, we captured a video. Here, the objective was to determine the

progress of local scouring and the inclination of the scale model due to local scouring and to measure the shape of the surface of the soil layer from three-dimensional (3D) data obtained using a digital camera. In addition, we used image data that met the duplication between images by more than 70%. The error in the 3D data was approximately 2 mm, which was different from the result measured by the laser displacement meter. Therefore, the inference is that using 3D data made it possible to qualitatively clarify the region of local scouring and the shape of the scour hole due to the changing angle. In addition, we measured the time at which the scale model was inclined and unable to stand on its own due to the water inflow at the surface of the soil layer.

## Effect on the Region of Local Scouring and Scour Depth Due to the Angle

The shape of the local scouring in case 1 is shown in Figure 7. At first, local scouring started near the diagonal upstream direction of the scale model, similarly to that observed in previous studies [15–18] for the cylindrical model (Figure 7(1)). Subsequently, local scouring proceeded towards the middle area in front of the pier upstream, and a local scour hole formed there (Figure 7(2)). The measurement results of the ground heights after the experiment in case 1 are shown in Figure 8. In addition, the rectangle shown in black in the figure is the installation location of the scale model, and the ground height at the start of the experiment was defined as 0 mm. The higher cases are shown as positive, and the lower cases are shown as negative. The maximum scour depth in front of the upstream scale model was 32.6 mm. The mean inclination angle of the scour hole in front of the scale model against the horizontal surface ($\phi$) was $25.1^{o}$. The local scouring upstream at the side of the scale model proceeded the same as at the front of the scale model. However, local scouring did not proceed in the downstream direction at the side of the scale model. This is because the flow along the scale model was underdeveloped downstream, and the downstream region became an accumulation region.

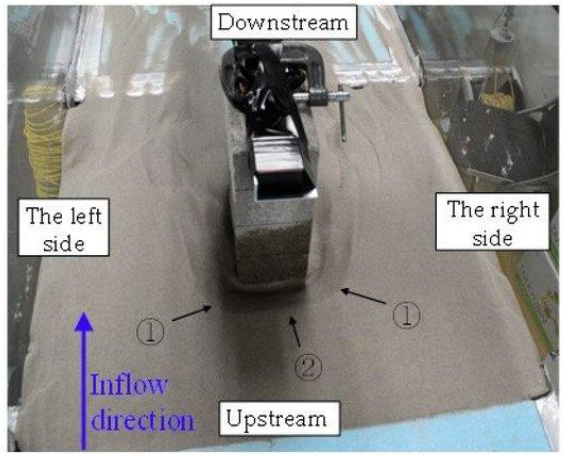


**Figure 7:** The shape of scouring (case 1).

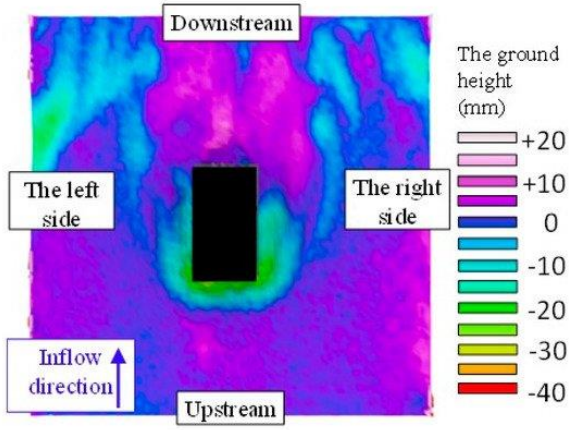


**Figure 8:** The measurement result of the ground height (case 1).

The shape of the local scouring in case 2 is shown in Figure 9. At first, the local scouring started at the upstream corner of the scale model on the right side facing downstream (Figure 9(1)). Next, local scouring started in the downstream and upstream corners of the scale model on the left side facing downstream (Figure 9(2)). Subsequently, local scouring proceeded towards the center of the short and long sides of the scale model and was sandwiched between the corners where it had initiated,

eventually forming a scour hole (Figure 9(3)). These tendencies are similar to those observed in a previous study [6]. The formation of the scour hole on the short side proceeded faster than that on the long side. In addition, we observed the condition of the winding up of sand near each corner where the local scouring proceeded, and the corner of the right side upstream was wound up the most, which is similar to results observed in a previous study [19]. The measurement results of the ground height after the experiment in case 2 are shown in Figure 10. We also used $\phi$ according to the focused direction. The maximum scour depth was 39.8 mm. $\phi$ was maximum at the right side upstream and decreased towards the left side downstream. This is because $\phi$ was changed due to the smaller scour depth in the other regions compared to that at the right upstream corner. However, for $\phi 1$, the reason is different. It is considered that $\phi 1$ was smaller than $\phi 2$ due to the increase in the horizontal distance of the scour hole according to the spread in the region affected by the down flow near the corner due to the angle. Focusing on the right side of the scale model in Figure 10, the scour depth (approximately 38 mm) was distributed approximately 40 mm in the direction perpendicular to the scale model axis direction. In the scale model axis direction, the scour region extended to near the center of the long side. It can be confirmed that scour progressed. In addition, the scour depth at each location advanced to a position deeper than the bottom of the scale model.

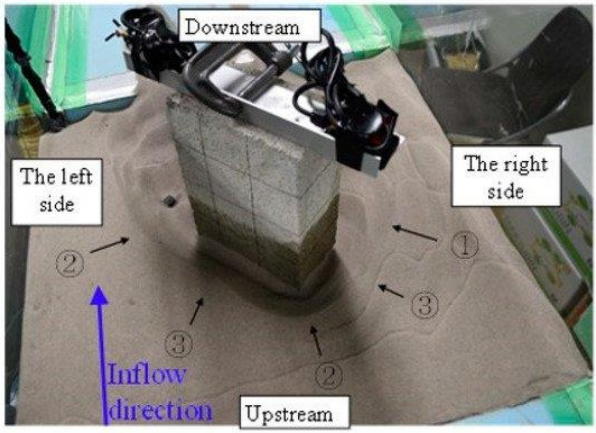


**Figure 9:** The shape of scouring (case 2).

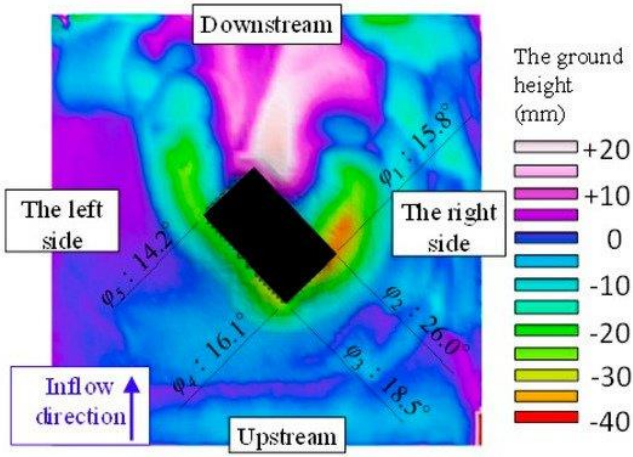


**Figure 10:** The measurement result of the ground height (case 2).

It can be observed that the wound-up sand accumulation region in case 2 was formed around the corner of the right side. It can also be observed that sand was accumulated the most on the flow direction line from the tip of the corner of the right side downstream, and the accumulation region was fan-shaped around this region. This is because the formed horseshoe [16–18,20] was distributed to create an angle to the direction of water flow along the short side or the long side of the scale model

facing upstream due to the angle θ. From these results, it can be observed that the scour region was widened from the upstream to the downstream of the pier through the angle of the center of the river flow against the pier. The scour depth near the corner on the downstream side of the left side tended to be smaller than that of the upstream side of the right side.

## Effect on the Inclination of the Pier Due to the Angle

The condition of the inclination during the experiment in case 3 is shown in Figure 11. The tendency of the progress of local scouring was similar to that in case 1. The scour hole formed because the local scouring on the upstream side proceeded to a position deeper than the bottom of the scale model, and the scale model was inclined. The scale model was gradually inclined after 135 s from the arrival of water at the surface of the soil layer in the upstream direction and was unable to stand on its own 163 s later in the upstream direction.

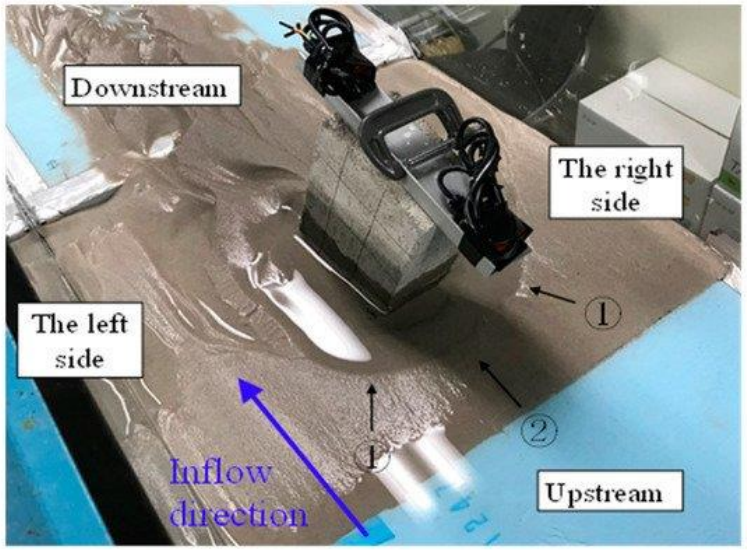


**Figure 11:** The condition of inclination during the experiment (case 3).

The condition of the inclination during the experiment in case 4 is shown in Figure 12. The tendency of the progress of scouring was similar to that in case 2. The scale model was gradually inclined 163 s from the arrival of water at the surface of the soil layer towards the upstream and the right side direction and was unable to stand on its own 215 s later in the same directions. The measurement result of the ground height is shown in Figure 13. The distribution of scouring was widened at the corner of the left side, downstream from the corner of the right side and upstream, and the scouring progress of the corner at the upstream right side proceeded the most. In addition, a fan-shaped accumulation region was formed near the corner of the downstream right side.

The tendency of the progress of scouring in case 5 was similar to that in cases 2 and 4. The scalemodel was gradually inclined 482 s from the arrival of water at the surface of the soil layer towards the upstream and right side directions and was unable to stand on its own 759 s later towards the same directions.

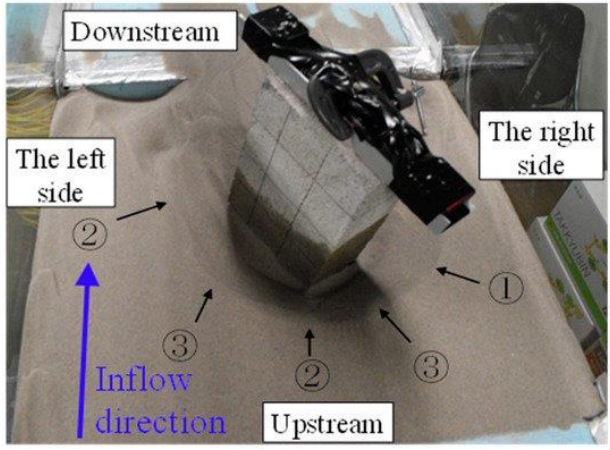


**Figure 12:** The condition of inclination during the experiment (case 4).

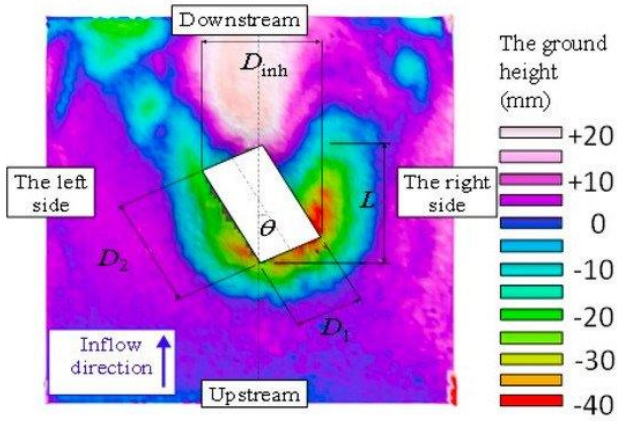


**Figure 13:** The measurement result of the ground height (case 4).

We focused on a length of the side of the scale model that inhibited water flow. $D_1$ is obtained when $\theta = 0$, $D_1 + D_2$ is obtained when $0 < \theta < 90$ and $D_2$ is obtained when $\theta = 90$. Therefore, given the range of $\theta$ from 0 to 90 degrees, the sum of the lengths of the sides that inhibit the water flow is always constant. However, the experimental results show that the scouring area and the time of occurrence of the pier inclined differently depending on the change in $\theta$. In addition, the Karman vortex generated downstream of the scale model is considered to have a different period and generation tendency depending on the fluctuation of $\theta$.

In this research, two-dimensional fluid numerical analysis was performed using FLOWSQUARE+(Made by "Nora Scientific", Tokyo, Japan), a form of numerical analysis software, for the purpose of grasping the characteristics of the flow around the scale model according to the fluctuation of $\theta$. An outline of the model for analysis is shown in Figure 14. The open channel and the scale model of the experiment are divided by an orthogonal grid with a grid point spacing of 5 mm. Analysis cases are shown in Table 2. The density of water is defined as 1000 kg/m$^3$, the kinematic viscosity coefficient of water is defined as $1.0 \times 10^{-3}$, and the flow velocity in the $X$ direction is defined as 0.03 m/s. $\theta$ is defined as 0, 30 and 45 degrees, as in the experiment. In addition, the case of $\theta$ as 90 degrees is also defined. In this research, we focused on the Strouhal number ($S_t$) obtained by

Equation (1), which is one of the indicators that characterizes the cyclically fluctuating unsteady flow,such as the Karman vortex.

$$S_t = f \times L/V, \quad (1)$$

where $S_t$ is the Strouhal number, $f$ is the frequency of the water flow, $L$ is the representative length and $V$ is the flow velocity in the $X$ direction. $f$ is the frequency of the Karman vortex obtained from the time history of the flow velocity in the Y direction generated downstream of the scale model. When $\theta$ is 0 and 90 degrees, the side that inhibits the water flow direction changes from $D_1$ to $D_2$ due to the fluctuation of $\theta$; however, each $S_t$ is approximately 0.1. These values are very close to the value obtained by other researchers [21,22]. On the other hand, $S_t$ is 0.293 when $\theta$ is 30 degrees, and $S_t$ is 0.281 when $\theta$ is 45 degrees. It can be seen that St increases by forming $\theta$. This is because the frequency of the Karman vortex increased due to the angle of the scale model with respect to the water flow direction. The contour diagram of the velocity distribution in the X direction at T = 10 s when $\theta$ is 45 degrees is shown in Figure 15. The Karman vortices are formed from near the corner on the upstream right side and the corner on the downstream left side, which are the ends of the $D_{inh}$, and the flow velocity in the vicinity is relatively small. In addition, we focused on the scour areas shown in Figures 10 and 13, and from the results of the experiment, the scour area is widely distributed upstream against the scale model from the corner of the upstream right side to the corner of the downstream left side, and each corner is the end of the $D_{inh}$. It can also be seen that the sedimentary area is distributed downstream against the scale model.

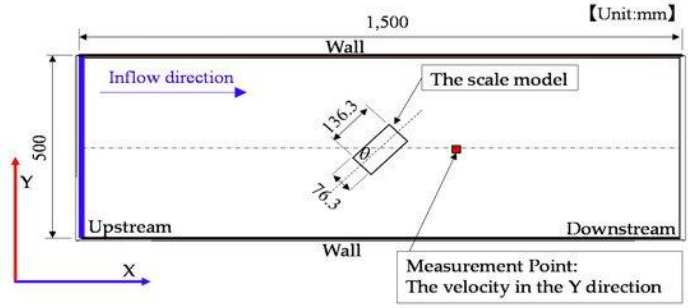


**Figure 14:** Outline of the model for analysis.

**Table 2:** Table of analysis cases.

| Case | $\theta$ (degree) | $D_1$ (mm) | $D_2$ (mm) | $L$ (mm) | $D_{inh}$ (mm) | Velocity (m/s) | $S_t$ |
|---|---|---|---|---|---|---|---|
| Ana0 | 0 | 76.3 | 136.3 | 136.3 | 76.3 | 0.03 | 0.140 |
| Ana30 | 30 | 76.3 | 136.3 | 156.2 | 134.2 | 0.03 | 0.293 |
| Ana45 | 45 | 76.3 | 136.3 | 150.3 | 150.3 | 0.03 | 0.281 |
| Ana90 | 90 | 76.3 | 136.3 | 76.3 | 76.3 | 0.03 | 0.132 |

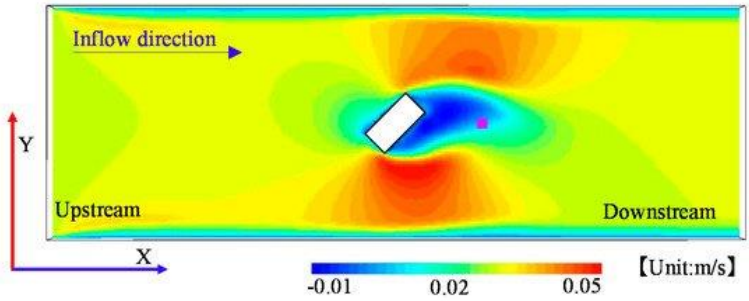


Figure 15: Contour diagram of the velocity distribution in the *X* direction at T = 10 s when $\theta$ is 45.

From these results, for water flow with an angle against the pier, it can be observed that $D_{inh}$ is more related to the formation of the scour region and the initiation of the pier inclination than the sum of the sides that hinder the flow of water. $D_{inh}$ can be geometrically expressed as:

$$D_{inh} = D_1 \times \cos\theta + D_2 \times \sin\theta, \qquad (2)$$

where $D_1$ and $D_2$ are the side lengths in the transverse and axis directions against the pier axis, respectively, and $\theta$ is the angle between the pier and the center of the river flow. The relationship between $D_{inh}$ and the water flow time T from the arrival of water at the surface of the soil layer is shown in Figure 16. In addition, in these experiments, the horizontal axis in Figure 16 was adjusted to a value obtained by dividing $D_{inh}$ by *F*r because the velocity was different in each experiment. The water flow time when initiating the scale model inclination and at the time when the model was unable to stand on its own is shown in Figure 16. When the value of $D_{inh}/Fr$ increases, it can be observed that the time of the initiation of the incline of the scale model and its inability to stand on its own increase. According to the previous research study by Ming-Hseng Tseng et al. [22], they have shown that the increase in the pressure coefficient in the upstream direction of the pier and decrease in the pressure coefficient in the downstream of the pier are higher in the square pier than in the cylindrical pier. In addition, St of the square pier [21,22] or "Ana0 and Ana90" is approximately 0.1,

that is smaller than 0.2 that is the general $S_t$ value around the cylindrical pier. From these results, it is considered that the horseshoe vortex that is formed around the pier is likely to be localized in the upstream side of the pier, when $S_t$ is decreased due to the frequency decrease of the Karman vortex which is formed by the water flow. Therefore, in the case of case 3 where $S_t$ is relatively small and q is 0, it is considered that time of the initiation of the incline of the scale model and its inability to stand on its own is the shortest due to the area of the scour being localized in the upstream side of the scale model. On the other hand, in the cases of case 4 and 5, where $S_t$ is increased with forming $\theta$, the scour region increased as the horseshoe vortex is distributed and the scale model began to incline and took the longest time to become unable to stand on its own. Therefore, when the center of the river flow is flowed in to form the angle against the pier, it can be observed that the initiation of the pier incline is late because the scour region widensand $D_{inh}$ increases.

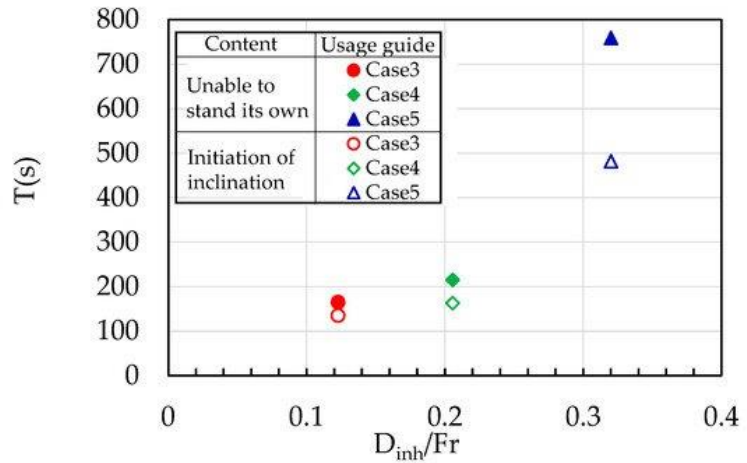


**Figure 16:** The relationship of $D_{inh}$ and the water flow time T from the arrival of water at the surface ofthe soil layer.

## Conclusions

In this research, we present an overview of the river flooding disaster in Japan in July 2018 and we have performed experiments using a scale model. The objectives of this study were to clarify the condition of the occurrence of scour

downstream around the pier and the influence on the progress of local scouring under these conditions. The results were as follows:

1. In the case that the center of the river flow forms an angle in respect to the pier, the scour region is widened from the upstream to the downstream of the pier because of its inhibition width, which is positioned in the transverse direction against the river flow.
2. The downstream scour depth is smaller than the upstream scour depth when the center of the river flow is at an angle to the pier.
3. When the center of the river flow flows to form an angle against the pier, the time of initiation of the inclination of the pier is increased according to the inhibition width.
4. When St is relatively small, the horseshoe vortex that is formed around the pier is localized on the upstream side of the pier. In addition, the time of the initiation of the incline of the scale model and its inability to stand on its own small is smaller than when St is relatively large due to the area of the scour being localized.

In this research, the effect of the angle between the river center and the pier was clarified as a condition for the downstream of the pier, but the inclination direction of the pier was different from that of the disaster case. The effect of accumulation can be considered as one of the factors, such as the driftwood from upstream at the time of the river flooding. This verification will be a subject of future research.

## References

1. Samizo M, Watanabe S, Sugiyama T, Okada K. Proposal of a statistical estimating method for scouring apprehended bridge piers under flood conditions. J. Jpn. Soc. Civ. Eng. Ser. D3 2013; 69: 237–249.
2. Keyaki T, Yuasa T, Naito N, Watanabe S. Soundness evaluation method of the ground around the pier foundation against scouring by microtremor measurements at both sides of the bridge piers. Jpn. Geotech. J. 2018; 13: 319–327.

3. Bento AM, Gomes A, Viseu T, Couto L, Pêgo JP. Risk-based methodology for scour analysis at bridge foundations. Eng. Struct. 2020; 223: 111115.
4. Yao W, Draper S, An H, Cheng L, Harris JM, et al. Effect of a skirted mudmat foundation on local scour around a submerged structure. Ocean Eng. 2020; 218: 108127.
5. Emmett ML. An analysis of relief bridge scour. J. Hydraul. Div. 1963; 89: 93–118.
6. Emmett ML, Toch A. Scour Around Bridge Piers and Abutments, HR-30 and Iowa Highway Research Board. The Iowa State Highway Commission and the Bureau of Public Roads. Ames, IA, USA. 1956.
7. Tarapore ZS. A Theoretical and Experimental Determination of the Erosion Pattern Caused by Obstructions in an Alluvial Channel with Particular Reference Circular Cylindrical Piers. Ph.D. Thesis, University of Minnesota. Minneapolis, MN, USA. 1962.
8. Suzuki K. Study on the Clear Water Scour around a Cylindrical Bridge Pier, Japan Society of Civil Engineers. Tokyo, Japan. 1981; 313: 47–54.
9. Melville BW, Raudkivi AJ. Effects of foundation geometry on bridge pier scour. J. Hydraul. Eng. 1996; 122: 203–209.
10. Richardson JE, Panchang VG. Three-dimensional simulation of scour-inducing flow at bridge piers. J. Hydraul. Eng. 1998; 124: 530–540.
11. Roulund A, Sumer BM, Fredsøe J, Michelsen J. Numerical and experimental investigation of flow and scour around a circular pile. J. Fluid Mech. 2005; 534: 351–401.
12. Cheng NS, Wei N. Scaling of scour depth at bridge pier base on characteristic dimension of large-scale vortex. Water. 2019; 11: 2458.
13. Manes C, Brocchini M. Local around structures and the phenomenology of turbulence. J. Fluid Mech. 2015; 779: 309–324.
14. Railway Technical Research Institute in JAPAN. Maintenance Standard (Railway Structure Edition, Foundation Structure and Retaining Structure). Railway Technical Research Institute in JAPAN. Tokyo, Japan. 2007; 165–171.
15. Umeda S, Yamazaki T, Ishida H. Time evolution of scour

and deposition around a cylindrical pier in steady flow. In Proceedings of the Fourth International Conference on Scour and Erosion. Tokyo, Japan. 5–7 November 2008; 140–146.
16. Umeda S, Yamazaki T, Masatoshi Y. Effects of foundation location on scour process around a cylindrical bridge pier. Ann. J. Hydraul. Eng. 2010; 54: 835–840.
17. Das S, Das R, Mazumdar A. Circulation characteristics of horseshoe vortex in scour region around circular piers. Water Sci. Eng. 2013; 6: 59–77.
18. Muzzammil M, Gangadhariah T. The mean characteristics of horseshoe vortex at a cylindrical pier. J. Hydraul. Res. 2003; 41: 285–297.
19. Briaud JL, Chen HC, Li Y, Nurtjahyo P, Wang J. Complex Pier Scour and Contraction Scour in Cohesive Soils, National Cooperative Highway Research Program. Transportation Research Board National Research Council. Washington, DC, USA. 2003.
20. Utami T. Study on horseshoe vortex around the pier. In Proceedings of the Annual Proceedings of JSCE, Hokkaido University, Hokkaido, Japan, 1–3 October 1973, Japan Society of Civil Engineers. Tokyo, Japan. 1973; 28: 226–227.
21. Durão DFG, Heitor MV, Pereira JCF. Measurements of turbulent and periodic flows around a square cross-section cylinder. Exp. Fluids. 1988; 6: 298–304.
22. Tseng MH, Yen CL, Song CCS. Computation of three-dimensional flow around square and circular piers. Int. J. Numer. Methods Fluids. 2000; 34: 207–227.